Kinetic Study of the Effect of Ethanol Addition on PAH and Soot Formation in Ethylene Flames

N.A.Slavinskaya[1], R. Whitside[1], J.H. Starcke[1], U. Riedel[1], D. Knyazkov[2,3], I.E. Gerasimov[2], O.P. Korobeinichev[2],

[1] *Institute of Combustion Technology, German Aerospace Centre (DLR), Pfaffenwaldring 38-40, 70569, Stuttgart, Germany*

[2] *Voevodsky Institute of Chemical Kinetics and Combustion, Institutskaya str. 3, Novosibirsk, 630090 Russia*

[3] *Novosibirsk State University, Pirogova str. 2, Novosibirsk 630090, Russia*

Abstract

The effects of ethanol (C_2H_5OH) addition to premixed laminar ethylene (C_2H_4) on polyaromatic hydrocarbon (PAH) and soot precursor formation is studied. The chemical kinetic mechanism, previously optimised using experimental data obtained in 30 different flames of methane, ethylene and ethane, was validated on mole fraction profiles recently measured in $C_2H_4/O_2/Ar$ and $C_2H_4/C_2H_5OH/O_2/Ar$ flames at low and atmospheric pressure. The simulations performed identify the kinetic effects of ethanol addition on the main precursor of benzene formation in premixed flames: reduction of the C_2H_3 production rate in ethylene/ethanol mixtures through a decrease of the H-atom abstraction reaction rate from C_2H_4, and through an exchange of C and H-atoms between intermediates produced during ethanol and ethylene oxidation. That leads to a decrease in concentrations of the main PAH precursors, such as C_2H_2, C_3H_x and C_4H_x.

Introduction

Practical fuels such as natural gas, gasoline, kerosene and diesel fuel are complex mixtures of hydrocarbons related mostly to three main families: *n*- or *i*- paraffins, naphthenes and aromatics. Oxygenated compounds are also used as additive extenders, oxygenates and renewable combustion fuels. The oxygen content in the fuel molecules generally decreases hazardous emissions, particularly PAHs (poly aromatic hydrocarbons), soot and CO.

The influence of oxygenated components in the fuel mixture on the formation of PAHs, the PAH precursors and soot, i.e. changes in reaction paths leading to aromatic molecules and soot particles, their growth and oxidation, are not highlighted enough despite intensive investigations [1-17]. The experimental studies [1-6, 8-17] performed for different fuels using different experimental devices demonstrate that addition of oxygenated compounds (mostly methanol, ethanol and methyl-tert-butyl ether) generally leads to reduction of soot formation, but depending on mixing conditions in diffusion flames, ethanol (C_2H_5OH) can be favourable to soot formation [5,16,17]. The number of modelling efforts to determine the kinetic mechanism of the influence of ethanol on soot formation is sufficiently small. Most of these works are related to liquid fuels [3,7,11].

The ethylene/ethanol system is best suited for studying the chemical effects of oxygenated compounds on the PAH and soot formation upon combustion of hydrocarbons. Ethylene is one of the most important intermediates formed during oxidation of hydrocarbons of different families and is actively involved in the reactions of formation of PAH precursors; ethanol is the most widely used biofuel. Combustion of ethylene/ethanol mixtures has been extensively investigated earlier [5, 6, 9-11,14-20].

The present paper focuses on the kinetic analysis of the influence of ethanol addition on PAH and soot formation in the flames of ethylene, an important intermediate for their formation in flames. The general aim is to understand the influence of oxygenated additives on soot production from hydrocarbon fuel combustion. In this work, early [6] and recent experimental data for premixed [12,13] flames are compared with numerical results based on a chemical kinetic model [21-25] developed to describe the behaviour of a large number of species relevant for PAH and soot formation. The simulations are performed using a well-established numerical code for modelling laminar diffusion flames which is capable of dealing with such a large mechanism [22-24]. This new data was used to improve the mechanism further. The main reaction paths leading to the aromatic molecule formation in flames with and without ethanol addition are analysed and discussed.

Kinetic model

The reaction kinetic model for C_2H_4/C_2H_5OH mixtures is derived from the global reaction database under constant development at the DLR Institute of Combustion Technology. The core detailed reaction model consists of a H_2/C_1-C_4 mechanism with PAH formation reactions [21-25]. The model extensions and improvements performed for the C_2H_2 and C_2H_5OH sub-mechanisms are described in [25].
The sub-mechanism for PAH formation was developed simultaneously with the base C_1-C_2 chemistry [22, 24]. Due to the absence of sufficient information regarding the thermochemical data for PAH related reactions, the reaction mechanism has be optimised based on the species concentration profiles obtained in 30 reference flames [21-25].

Modelling results

In this section the validation of the mechanism against experimental data on species and soot mole fraction profiles in laminar premixed burner-stabilized flames at low (30 torr) [12] and atmospheric pressure [6,13] is presented.
Numerical modelling was performed using the PREMIX code from the CHEMKIN II package [26]. For soot volume fraction predictions, a modified version [27] of the original soot model of Wang & Frenklach [28] has been used, whose main feature is the implementation of detailed PAH chemistry into the coagulation and surface growth modules, allowing for the selection of a set of PAHs involved in soot inception by PAH coagulation [57]. In our simulations, all PAHs with a mass between 202 amu (A4) and 252 amu (BAPYR) were selected to form soot particles by coagulation.
The calculations of the species mole fraction profiles in low-pressure ethylene and ethylene/ethanol flames were first performed using the temperature profiles provided in [12]. These temperature profiles were derived by Korobeinichev et al. [12] from their experimental temperatures (measured by a thermocouple at 15 mm from the sampling probe tip), lowered by 100 K and shifted 3.5 mm away from the burner surface in order to take into account the thermocouple's temperature disturbance caused by the probe's cooling effects. However, calculations with these temperature profiles showed inadequate reproduction of the behaviour of mole fractions of some intermediates (C_3H_4, C_3H_5, C_4H_2, C_4H_6) downstream of the active reaction zone. This could be associated with errors in the determination of the actual temperature in the flame. In fact, the authors of [12] did not measure the temperature directly in the vicinity of the sampling probe's tip, but away from it with a subsequent application of a special procedure to make the temperature profile corrections for the flame cooling effect by the probe. This motivated us to modify the temperature profiles provided by the authors of

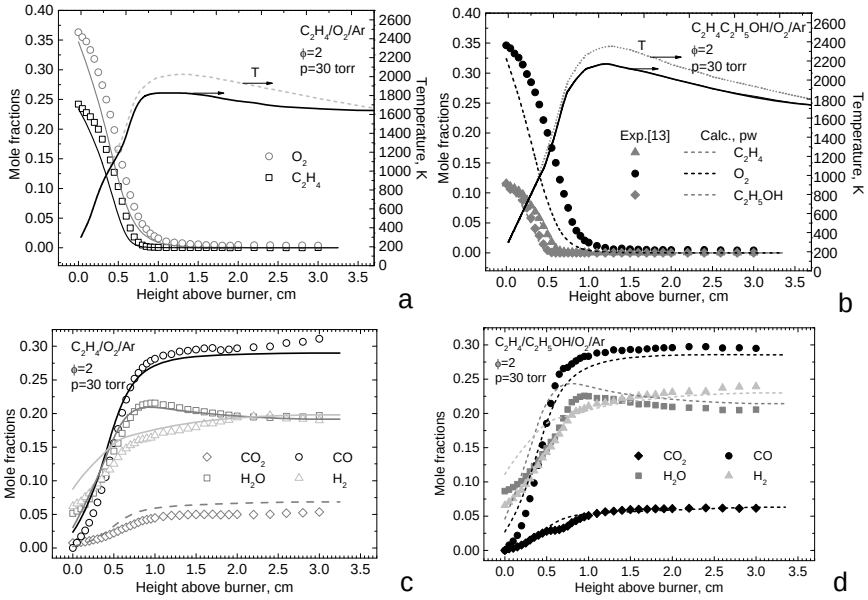

Figure 1. Mole fraction profiles of reactants and major products in a,c) pure ethylene and b,d) 50%C_2H_4/50%C_2H_5OH/O_2/Ar flames at p=30torr, $\phi = 2$. Symbols: experiment [12]; lines: modelling using mechanism [25]. Short dashed and dot temperature profiles are not corrected experimental data.

[12] by lowering their maximum temperatures by about 200 K. This alteration of the temperature profile in our simulations did not result in any significant changes in the maximum mole fractions of the studied species (in comparison with the calculations using the temperature provided in [12]), but allowed for the correct description of the mole fraction behaviour of some species in the post-flame zone.

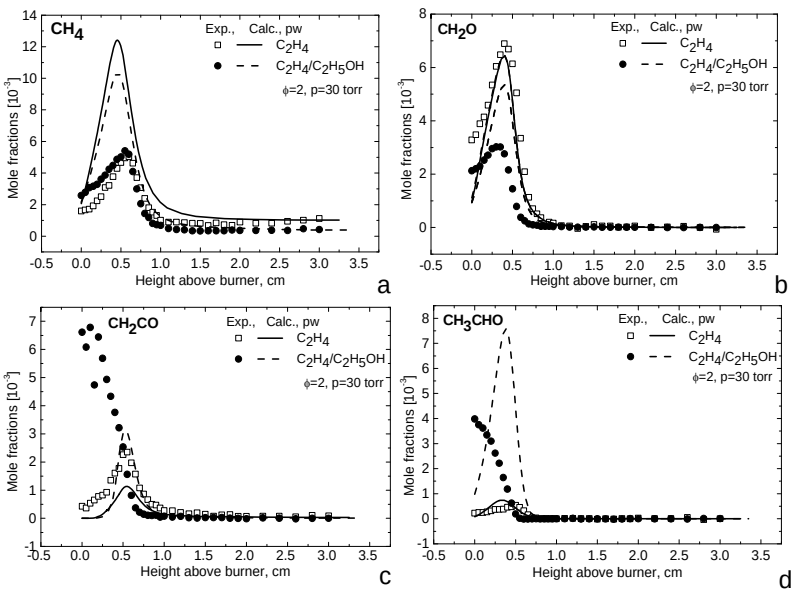

Figure 2. Mole fraction profiles of major intermediate products in pure ethylene and ethylene/ethanol flames at p=30torr, $\phi = 2$. Symbols: experiment [12]; lines: modelling using mechanism [25]. Open symbols and solid lines are for C_2H_4/O_2/Ar flame, filled symbols and dashed lines correspond to 50%C_2H_4/50%C_2H_5OH/O_2/Ar.

Fig. 1-4 compare the simulated species mole fraction profiles with those measured by Korobeinichev et al. [12] in premixed, burner-stabilized, ethylene/oxygen/argon flames with and without ethanol at low-pressure conditions. In Fig. 1a and 1b temperature profiles reported in [12] and those modified (and used) in this work are shown. The measured height above the burner was not corrected in the modelling. The uncertainties in the measurements of absolute mole fractions of the flame species were not reported by the authors [12], however, as per private communication with them, were reported to have an uncertainty of a factor of 2-3 for intermediate species and ±15% for reactants and major flame products (CO, CO_2, H_2, H_2O). The uncertainties indicated above are mainly due to the calibration errors and the errors in the values of the ionization cross sections used for converting the signal intensities into the mole fractions of intermediates.

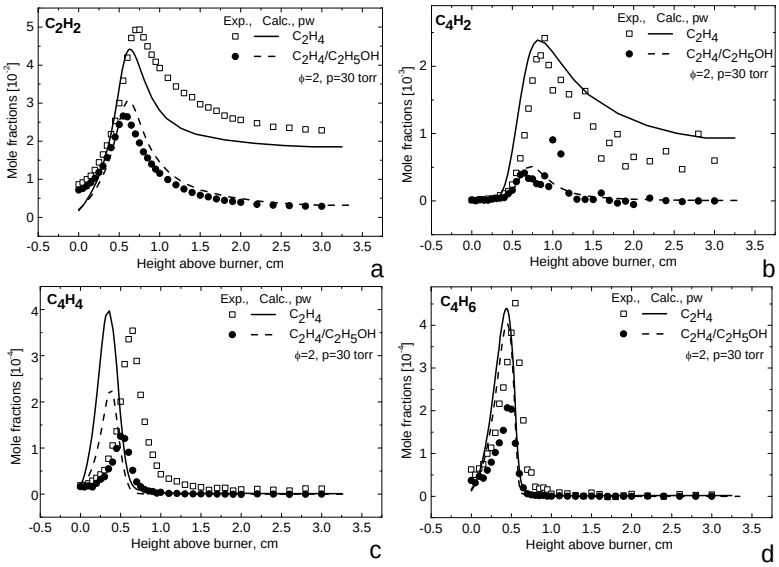

Figure 3. Mole fraction profiles of acethylene and the major intermediate C_4 products in pure ethylene and ethylene/ethanol flames at p=30torr, $\phi = 2$. Symbols: experiment [12]; lines: modelling using mechanism [25]. Open symbols and solid lines are for $C_2H_4/O_2/Ar$ flame, filled symbols and dashed lines correspond to $50\%C_2H_4/50\%C_2H_5OH/O_2/Ar$.

In Fig. 1 the simulation results of reactants (C_2H_4, O_2, and C_2H_5OH) and major stable products (CO, CO_2, H_2, H_2O) measured in the ethylene flames [12] with and without ethanol are shown. The computed results are in good agreement with measurements [12] and indicate that replacing 50% of ethylene with ethanol in the fresh mixture does not lead to a change in the final composition of products: the mole fractions of CO_2, H_2O, CO and H_2 are approximately similar in values and trends for both investigated low-pressure flames.

Measured [12] and simulated concentration profiles of intermediate molecules CH_4, CH_2O, CH_2CO, CH_3CHO, C_2H_2, C_4H_2, C_4H_4, C_4H_6 and radicals, C_3H_3, C_3H_4 and C_3H_5, involved in aromatic ring formation, as well as the aromatic molecule benzene, C_6H_6, are shown in Fig. 2, 3 and 4.

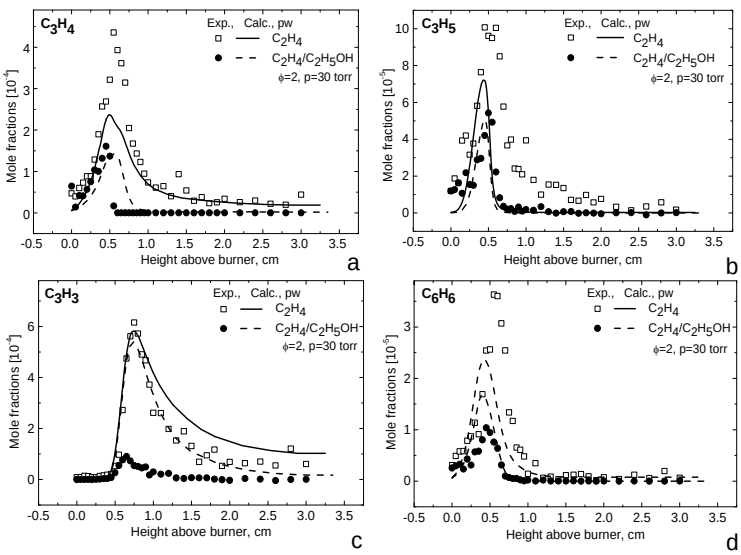

Figure 4. Mole fraction profiles of major C_3 radicals, methyl and benzene in pure ethylene and ethylene/ethanol flames at p=30torr, $\phi = 2$. Symbols: experiment [12]; lines: modelling using mechanism [25]. Open symbols and solid lines are for $C_2H_4/O_2/Ar$ flame, filled symbols and dashed lines correspond to $50\%C_2H_4/50\%C_2H_5OH/O_2/Ar$.

The modelling results are consistent with the experimental concentrations of CH_2O and CH_3CHO obtained in pure ethylene flames and over-predict these concentrations for ethylene/ethanol flames, Fig. 2b and 2d, with a factor of 1.5-1.8. The predicted methane concentrations are 2-2.5 times higher than the measured data. Ketene, CH_2CO, is under-predicted in the model by a factor of 2 for both flames. The experimental and simulated results coincide generally well in trends: concentrations of the main oxygenated products of ethanol oxidation, CH_2CO and CH_3CHO, Fig. 2c and 2d, are sufficiently higher in the ethylene/ethanol flame. The decrease of CH_2O concentration observed experimentally in ethylene/ethanol flames, Fig. 2b, is questionable and can be related to experimental uncertainty.

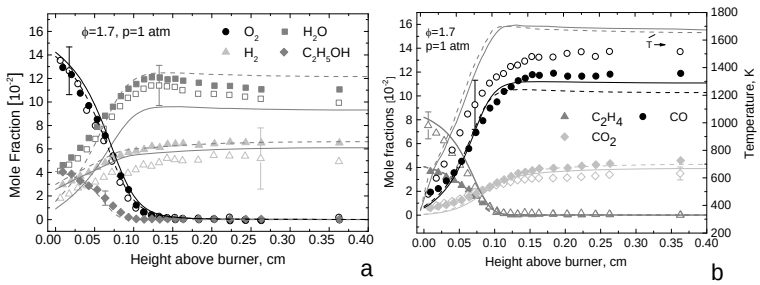

Figure 5. Mole fraction profiles of reactants and major products in pure ethylene and ethylene/ethanol flames at p=1atm, $\phi = 1.7$. Symbols: experiment [13]; lines: modelling using mechanism [25]. Open symbols and solid lines are for $C_2H_4/O_2/Ar$ flame, filled symbols and dashed lines correspond to 50%C_2H_4/50%$C_2H_5OH/O_2/Ar$. Bonds are experimental errors.

The comparision of modelled and experimental data for acetylene, diacetylene, vinylacetylene and 1,3,-butadiene, which are very important for PAH molecule formation and soot growth, are shown in Fig. 3a-d. The data demonstrate a strong agreement in trends and values. Concentrations of C_4H_4 and C_4H_6 for the ethylene/ethanol flame are over-predicted by a factor of 2. Concentrations of C_2H_2, C_4H_2, C_4H_4 and C_4H_6, Fig. 3a-d, decrease with ethanol addition.

The model demonstrates good reproducing experimental data for C_3H_4, C_3H_5 and C_6H_6 for ethylene/ethanol flame and and undepredicts these data for pure ethylene flame, Fig.4. The calculated C_3H_3 concentration is in agreement with measurements in ethylene flame, but the 6 fold decrease of propargyl concentration in the ethylene/ethanol experimental flame is not supported by modelling, Fig.4c. Also the trends in the C_3H_4 and C_3H_5 concentration behaviour, which are bound with reactions of the C_3H_3 production, do not support the measured data for the C_3H_3 profile, Fig. 4. The observed 3 fold decrease in benzene formation, Fig. 4d, generally reproduced by the model, could not be related only to propargyl recombination, but also to other reactions of aromatic ring cyclisation. That will be analysed in the next part of paper.

The simulations of data measured in atmospheric $C_2H_4/O_2/Ar$ and $C_2H_4/C_2H_5OH/O_2/Ar$ flames [13] are shown in Fig. 5-7 for an equivalence ratio $\phi = 1.7$. All of the simulations were performed using the temperature profiles provided by the authors of [13].

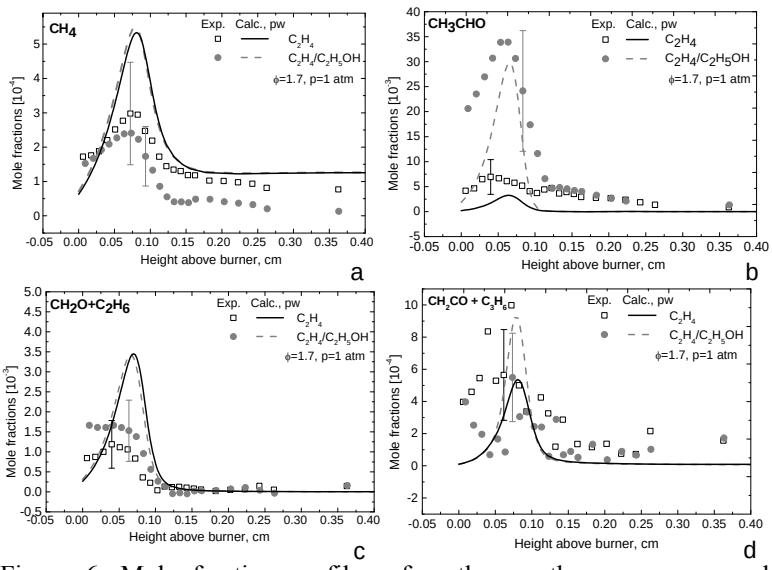

Figure 6. Mole fraction profiles of methane, ethane, propene and oxygenated species in pure ethylene and ethylene/ethanol flames at p=1atm, $\phi = 1.7$. Symbols: experiment [13]; lines: modelling using mechanism [25]. Open symbols and solid lines are for $C_2H_4/O_2/Ar$ flame, filled symbols and dashed lines correspond to 50%C_2H_4/50%$C_2H_5OH/O_2/Ar$. Bonds are experimental errors.

Measured and simulated mole fractions of reactants (C_2H_4, O_2, C_2H_5OH) and major products (CO, CO_2, H_2, H_2O) in flames with and without ethanol at $\phi = 1.7$ are shown in Fig. 5. The reaction mechanism reproduces the mole fraction profiles of each species well, along with an increase in the mole fractions of CO_2, H_2O and H_2 and a decrease in the CO mole fraction through replacing 50% of ethylene with ethanol in the fresh mixture.

Some disagreement can be observed only for carbon monoxide in the post-flame zone. But the authors of [13]

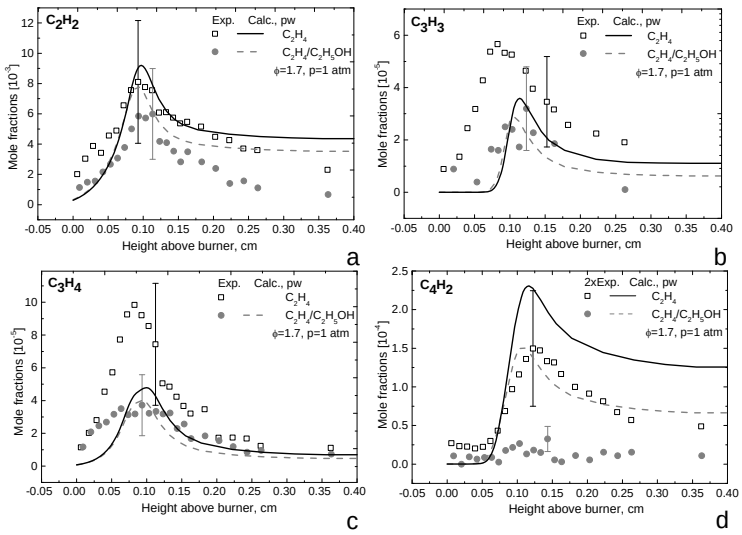

Figure 7. Mole fraction profiles of C_3–C_4 hydrocarbon intermediates in pure ethylene and ethylene/ethanol flames at p=1atm, ϕ=1.7. Symbols: experiment [13]; lines: modelling using mechanism [25]. Open symbols and solid lines are for $C_2H_4/O_2/Ar$ flame, filled symbols and dashed lines correspond to 50%C_2H_4/50%$C_2H_5OH/O_2/Ar$. Bonds are experimental errors.

pointed towards the higher measurement error of the CO mole fractions in this zone, because carbon-containing products other than CO and CO_2 were not taken into account by the determination of the carbon material balance in the post-flame zone.

Results of modelling the mole fraction profiles of methane, ethane, propene and oxygenated species and of aromatic precursors C_3H_4, C_3H_3 and C_2H_2 from [13] are shown in Fig. 6 and Fig. 7. Reasonable agreement with data [13] has been reached for CH_3CHO, C_2H_2, C_3H_3, and C_3H_4 species. The biggest discrepancies between experimental and simulated data have been obtained for concentrations of CH_4, combination of CH_2O+C_2H_6 (factor of 2-3, both flames), and C_4H_2 (factor of 4 in ethylene/ethanol flame), Fig. 6a, c and Fig. 7d. It was impossible to improve this over-prediction without worsening the results of simulations of formaldehyde and diacetylene in other experiments collected in Table 1. The discrepancies with other measured concentration profiles do not exceed the given experimental errors.

The experiment shows a slightly lower methane mole fraction in the flame with ethanol throughout the whole flame zone than that in the pure ethylene flame, Fig. 6a. That contradicts experimental results obtained for methane concentration in flames [12], Fig. 2a, and with simulation data obtained with the present reaction mechanism; the model predicts an increase of methane mole fraction in the ethylene/ethanol flame. The same trend was demonstrated by 3 different mechanisms, which were used in [13] for simulation of measured results.

A sensitivity analysis showed that the concentration of CH_4 in the 50%C_2H_4/50%C_2H_5OH flame is mostly influenced by reactions:

$C_2H_5OH+H \Leftrightarrow CH_2CH_2OH+H_2$ (R1)
$C_2H_5OH+CH_3 \Leftrightarrow CH_2CH_2OH+CH_4$ (R2)
$C_2H_5OH+CH_3 \Leftrightarrow CH_3CHOH+CH_4$ (R3)
$CH_4+OH \Leftrightarrow CH_3+H_2O$ (R4)
$CH_3+HCO \Leftrightarrow CH_4+CO$ (R5)
$CH_2O+CH_3 \Leftrightarrow CH_4+HCO$ (R6)

Only reactions (R1-R3) were optimised in [25] and in our present work. This optimisation has been performed through simulation of experimental investigations [12,13, 29-33] and reaction path analysis performed for these systems. As a result of this analysis, the reaction rate coefficient for (R2) adopted from [34] has been reduced by a factor of 5. Analysis of the computed flame structures reveals that modifications in the rate coefficients (R1) and (R3) do not result in a change of methane concentration or lead to unacceptable alterations in the

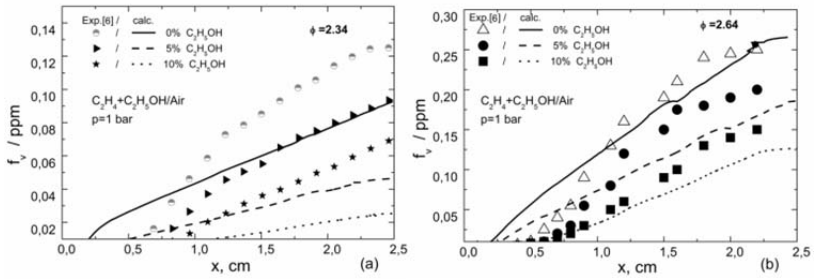

Figure 8. Comparison of measurements [6] (symbols) and simulations (lines) for soot in flames of pure ethylene and ethylene doped with 5% and 10% ethanol; p=1bar, ϕ =2.34 and 2.64.

concentrations of H_2CO, CH_2CO and CH_3CHO, laminar flame speed and ignition delay time simulations for methane and ethanol. This means either the mechanisms do not reproduce the effect of the ethanol addition on the methane mole fraction in the flame [13] or there is a problem with the consistency of the experimental data. In either case, the concentration profiles for CH_4, H_2CO and CH_2CO measured in flames [12] and [13] demonstrate contradictory trends for ethanol addition to ethylene. The concentration of CH_4 is not influenced by ethanol addition in flame [12] and decreases in flame [13]; H_2CO decreases in [12] and increases in [13]; CH_2CO increases in [12] and decreases in [13].

Through reaction path analysis, concentrations of CH_4, H_2CO and CH_2CO in ethanol flames are approximately 1.3-3 times higher than in the ethylene flames, mainly due to the greater production of CH_3CHO and CH_3CO.

Fig. 8 demonstrates simulations of the soot concentration profiles measured in a flat-flame burner at equivalence ratios of 2.34 and 2.64 studied in [6]. Ethanol was added to ethylene at two levels corresponding to 5% and 10% oxygen by weight in the fuel. The simulations under-predict the soot volume fractions in flames with $\phi = 2.34$ and match reasonably well experiments with $\phi = 2.64$. Despite uncertainties in the temperature measurements and in the soot model, which contribute to the modelling difficulties, obtained results reflect the values and trends in soot formation with changes in equivalence ratio and ethanol concentration in the fuel: addition of ethanol to the ethylene reduces the amount of soot particles proportional to the amount observed experimentally.

REACTION PATH ANALYSIS

Sensitivity and reaction path analyses have been performed for the analysed flames, Figures 1-8. To identify the main reaction steps leading to cyclization of the first aromatic ring (A1, benzene), flames have been analysed at two different temperatures: at the beginning of the reaction zone, at 600 K, and in the developed reaction zone, at 1550 K. These temperatures also define the different regimes, i.e. low- and high-temperature paths, of the aromatic ring formation [21,34].

For investigated flames, independent of pressure, temperature and equivalence ratios, the most important cyclization reactions, are:

$H_2CCCCH+C_2H_2$<=>A1- (R7)
i-$C_4H_5+C_2H_2$<=>A1+H (R8)
$C_2H_3+C_4H_4$<=>A1+H (R9)
$H_2CCCCH+C_2H_3$<=>A1 (R10)
$2H_2CCCH$<=>A1 (R11)
$2H_2CCCH$<=>A1-+H (R12)

Reactions of propargyl recombination become important at high temperature, in the main reaction and in the post-flame zones.
Note, that notations H_2CCCCH and i-C_4H_5 are used for lumped isomers of C_4H_3 and C_4H_5 [21].
The A1 concentration has the highest sensitivity coefficient in all investigated flames to reaction

$C_2H_3+O_2 <=> CH_2O+HCO.$ (R13)

This coefficient is negative: consumption of C_2H_3 in oxidation reaction (R13) reduces the benzene production rate directly in reactions (R9, R10), and indirectly through reactions (R7, R8) due to a decrease in the acetylene and i-C_4H_5 rate production

$C_2H_3+O_2 <=> C_2H_2+HO_2$ (R14)
i-C_4H_5 $<=> C_2H_2+ C_2H_3$ (R15)

Acetylene and i-C_4H_5 promote C_4H_4, C_4H_3, C_4H_2 and C_3H_3 formation, which further participate in the cyclization reactions.
The main channels of C_2H_3 production in pure ethylene and ethanol blended flames are

$C_2H_4+OH <=> C_2H_3+H_2O$ (R16)
$C_2H_4+H <=> C_2H_3+H_2.$ (R17)

In mixtures with C_2H_5OH, reactions (R16) and (R17) compete with (R1) and

$C_2H_5OH+H <=> CH_3CHOH+H_2$ (R18)
$C_2H_5OH+OH <=> CH_3CHOH+H_2O$ (R19)
$C_2H_4+OH <=> CH_3CHO+H$ (R20)
$C_2H_4+OH <=> CH_2O+ CH_3.$ (R21)

Reactions (R18-R21) consume radicals H and OH and decrease by that the reaction rates of (R16-R17), consequently (R7-R15), and therefor A1 concentration.
Reaction (R1) promotes benzene production through accelerating the formation of OH radicals in

$CH_2CH_2OH+O_2 <=> 2CH_2O+OH,$ (R22)

while reactions (R18) and (R19) have an additive negative effect on A1 formation through formation of CH_3CHOH radical, leading to the more stable CH_3HCO.
Also, the negative effect of

i-$C_4H_5+O_2 <=> CH_2CO+CH_2HCO$ (R23)

on A1 production in mixtures containing ethanol appears at 600 K. This reaction competes with reactions of benzene production from C_4H_x at lower temperature.
The performed analysis allows selecting the kinetics factors, i.e. reaction paths, leading to reduction of the PAH and soot precursors in all investigated flames. Fig. 9 highlights the additive reaction paths to benzene formation compared to the pure ethylene case, which is caused by the kinetics of the process and not by the effects of a change in C/O ratio. The key

component in the reaction sequence to PAHs is C_2H_3. Its rate of production and concentration can be reduced in ethylene/ethanol mixtures through a) decrease of H-atom abstraction reaction rate from C_2H_4, as H and OH radicals are also involved in the reactions of C_2H_5OH with production of smaller oxygenated radicals and molecules; and b) through an exchange of C and H-atoms between intermediates produced at ethanol and ethylene oxidation pathways.

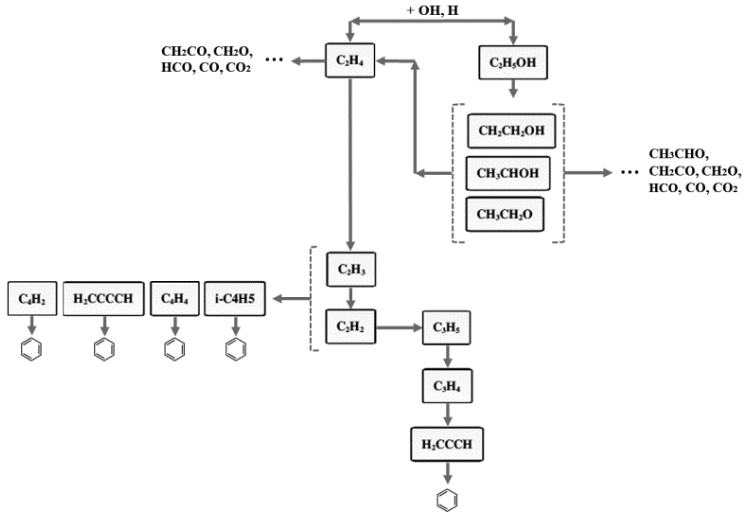

Figure 18. Principal integrated kinetic scheme of benzene formation in C_2H_4/C_2H_5OH mixture

The main effect of the C/O ratio is obvious: the smaller C/O ratio accelerates the reactions of the PAH precursors with O_2, O, OH and HO_2. That leads to formation of oxygenated molecules instead of aromatic cyclization. So, through a higher concentration of HO_2 the consumption of C_3H_5 grows in reactions

$C_3H_5+HO_2 \Rightarrow C_2H_3+CH_2O+OH$

$C_3H_5+HO_2 \Leftrightarrow OH+HCO+C_2H_4$

and leads to decreasing concentrations of C_3H_4 and C_3H_3.

The secondary channel of C_3H_5 production also needs to be mentioned. In the mixtures with higher C/O ratios, it can be formed in the sequence starting with butane formation: $C_3H_8=CH_3+C_2H_5 \rightarrow C_3H_7=C_3H_6+H \rightarrow C_3H_7+O_2=C_3H_6+HO_2 \rightarrow C_3H_6+OH=C_3H_5+H_2O$. The smaller the C/O ratios, the smaller the contribution of this channel is in C_3H_5 and finally in C_3H_3 production.

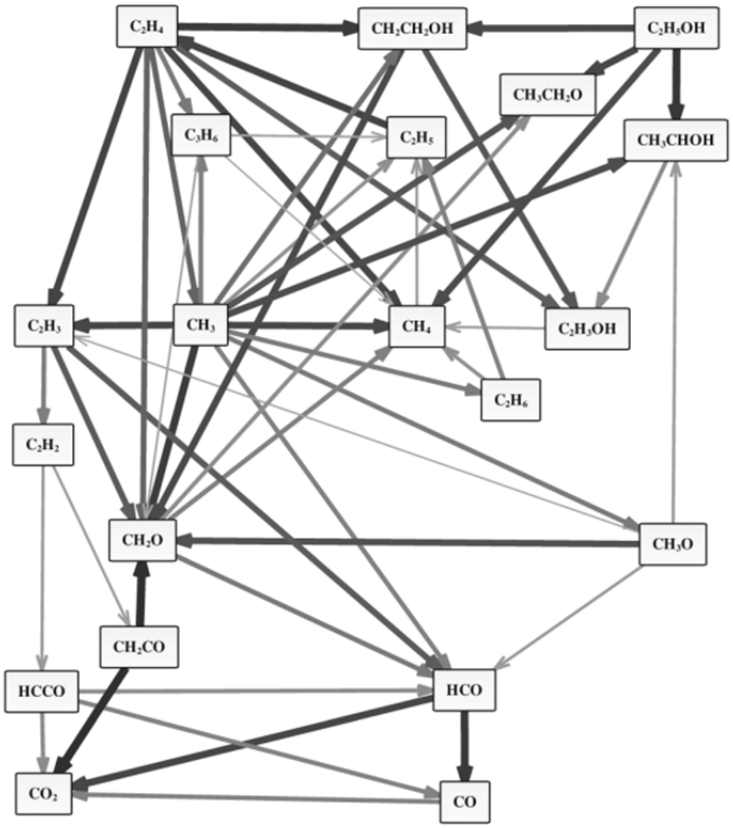

Figure 10. Atom flux diagram for $50\%C_2H_4/50\%C_2H_5OH/O_2/Ar$ flame [13] at T=1300K.

The carbon atom flow diagram (produced with Software Chemical Workbench [35]), Fig. 10, derived for the

50%C_2H_4 &50% C_2H_5OH flame [13] at 1300 K, highlights the complicated communication between intermediates produced at ethylene and ethanol oxidation.

CONCLUSIONS

The study investigates the influence of ethanol on the reaction paths of PAH and soot precursor formation in ethylene premixed flames. The chemical kinetic mechanism, previously optimised using experimental data obtained in 30 different flames of methane, ethylene and ethane was applied for the simulations of concentration profiles of stable species, intermediate radicals, benzene and soot in premixed burner-stabilized flames at low and atmospheric pressure. Comparison of the computed and measured species concentration profiles demonstrate that the model describes well the structure of the flames and correctly predicts values and general trends in species concentration. The quantitative disagreement for some species can be explained by the uncertainties in kinetic and experimental data. The simulated data studied in this paper disagrees with experimental data in the worst case (combination of CH_2O+C_2H_6 and C_4H_2 for some flames) by a factor 4. Recently published experimental data [12,13] is consistent with earlier published data and the applied reaction mechanism for PAH formation. The need of the methods for the evaluation of experimental data consistency is demonstrated.
Both experimental and modelling results indicate that ethanol contributes to suppression of the main PAH precursors and soot formation in premixed laminar flames. Analysis of the main pathways of the reactions leading to benzene formation in premixed flames has shown that soot reduction in the ethylene/ethanol flame occurs due the reduction of the C_2H_3 formation when a portion of ethylene is replaced with ethanol in the initial combustible mixture.

References

1. M. Frenklach, T. Yuan, Proc. International Symposium on Shock Tubes and Waves 16 (1987) 487.
2. A. Alexiou, A. Williams, Combust. Flame 104 (1996), 51-65.
3. P.F. Flynn, A.O. Zur Loye, F.L. Dryer, W.J. Pitz, C.K. Westbrook, E.M. Fisher, H.J. Curran, O.C. Akinyemi, D.W. Layton, P.A. Glaude, N.M. Marinov, R.P. Durrett, 2001. Detailed chemical kinetic modeling of diesel combustion with oxygenated fuels. SAE Technical Paper 2001-01-0653. Inal Senkan, 2002
4. K.H. Song, P. Nag, T.A. Litzinger, D.C. Haworth, Combust. Flame 135 (2003) 341-349.
5. K.L. McNesby, A.W. Miziolek, T. Nguyen, F.C. Delucia, R.R. Skaggs, T.A. Litzinger, Combust. Flame 142 (2005) 413-427.
6. J. Wu, K.H. Song, T. Litzinger, S.Y. Lee, R. Santoro, M. Linevsky, M. Colket, D. Liscinsky, Combust. Flame 144 (2006) 675-687.
7. C.K. Westbrook, W.J. Pitz, H.J. Curran, J. Phys. Chem. A. 110 (2006), 6912-6922.
8. A. Santamaria, E. G. Eddings, F. Mondragon, Combust. Flame 151 (2007) 235-244.
9. C. McEnally, L. D. Pfefferle, Proc. Combust. Inst. 31 (2007) 603-610.
10. B.A.V. Bennett, C.S. McEnally, L.D. Pfefferle, M.D. Smooke, M.B. Colket, Combust. Flame 156 (2009) 1289-1302.
11. R.J. Therrien, A. Ergut, Y.A. Levendis, H.Richter, J.B. Howard, J.B. Carlson, Combust. Flame 157 (2010) 296–312.
12. O.P. Korobeinichev, S.A. Yakimov, D.A. Knyazkov, T.A. Bolshova, A.G. Shmakov, J. Yang, F. Qi, Proc. Combust. Inst. 33 (2011) 569-576.

13. I.E. Gerasimov, D.A. Knyazkov, S.A. Yakimov, T.B. Bolshova, A.G. Shmakov, O.P. Korobeinichev, Combust. Flame 159 (2012) 1840-1850.
14. M. Salamanca, M. Sirignano, M. Commodo, P. Minutolo, A. D'Anna, Exp. Therm. Fluid Sci. 43 (2012) 71-75.
15. M. Salamanca, M. Sirignano, A. D'Anna, Energy & Fuels 26 (2012) 6144-6152.
16. J. Appel, H. Bockhorn, M.Y. Frenklach, Combust. Flame 121 (2000) 122–136.
17. N.M. Marinov, Int. J. Chem. Kinet. 31 (1999) 183−220.
18. H. Wang, X. You, A.V. Joshi, S.G. Davis, A. Laskin, F. Egolfopoulos, C.K. Law, USC Mech Version II. High-temperature Combustion Reaction Model of H2/CO/C1-C4 Compounds, 2007. <http://ignis.usc.edu/USC_Mech_II.htm>.
19. A.A. Konnov, Combust. Flame 156 (2009) 2093–2105.
20. T. Ni, S.B. Gupta, R.J. Santoro, Proc. Combust. Inst. 25 (1994) 585-592.
21. N.A. Slavinskaya, P. Frank, Combust. Flame 156 (2009) 1705-1722.
22. S.B. Dworkin, Q. Zhang, M.J. Thomson, N.A. Slavinskaya, U. Riedel, Combust. Flame 158 (2011) 1682–1695.
23. N.A. Slavinskaya, U. Riedel, S.B. Dworkin, M.J. Thomson, Combust. Flame 159 (2011) 979–995.
24. V. Chernov, M.J. Thomson, S. B., N.A. Slavinskaya, U. Riedel, Combust. Flame 161 (2014) 592–601.
25. N.A. Slavinskaya, R. Whitside, U. Riedel, Combust. Flame, submitted.
26. R.J. Kee, F.M. Rupley, J.A. Miller, Chemkin-II: a FORTRAN chemical kinetics package for the analysis of gas phase chemical kinetics, Report No. SAND89-8009B, Sandia Laboratories Report, 1993.
27. H. Böhm, M. Braun-Unkhoff, P. Frank, Progress in Computational Fluid Dynamics 3 (2003) 145-150.
28. M. Frenklach, H. Wang, in: H. Bockhorn (Ed.), Detailed Mechanism and Modeling of Soot Particle Formation, Springer-Verlag, Berlin, 1994, Vol. 59, p. 165.
29. M. Aghsaee, S.H. Dürrstein, J. Herzler, H. Böhm, M. Fikri, C. Schulz, Combust. Flame 161 (2014) 2263–2269.
30. A. Lamprecht, B. Atakan, and K. Kohse-Höinghaus, Combust. Flame 122 (2000) 483-491.
31. T.S. Kasper, P. Oßwald, M. Kamphus, K. Kohse-Höinghaus, Combust. Flame 150 (2007) 220-231.
32. N. Leplat, P. Dagaut, C. Togbe, J. Vandooren, Combust. Flame 158 (2011) 705-725.
33. N. Leplat, J. Vandooren, Comb. Sci. and Tech. 182 (2010) 436-488.
34. Z. F. Xu, J. Park, and M. C. Lin, J. Chem. Phys. 120, (2004) 6593- 6599.
35. Kintech Lab Ltd., Chemical Workbench®, http://www.kintechlab.com/, 2017.